



14th IEA Heat Pump Conference
15-18 May 2023, Chicago, Illinois

Innovative small capacity gas driven ammonia-water absorption heat pump prototype for space heating and domestic hot water production

Pistocchini Lorenzo ^{a,*}, Villa Giorgio ^a, Paulin Cesare ^a, Toppi Tommaso ^a

^aPolitecnico di Milano, via G. La Masa 34, Milan 20156, Italy

Abstract

Gas driven absorption heat pumps are a viable alternative for efficient space heating and domestic hot water production in residential and light commercial buildings with high temperature distribution systems. This work presents a second-generation ammonia-water absorption heat pump prototype, with patent-pending components developed by Politecnico di Milano. The innovative design of desorber and rectifier improves the heat and mass transfer in the generator whilst reducing its height and complexity. All the heat exchangers, except for the generator, are plate heat exchanger and a specifically designed oil driven diaphragm pump is used as solution pump. The overall weight of the prototype, excluding the continuous fin-type outdoor heat exchanger, is kept below 70 kg for a unit with nominal capacity of 10 kW. Variable restrictors for both solution and refrigerant branches are used to improve part load operation and the seasonal efficiency. Laboratory tests confirm high performance over a supply water temperature range between 25 °C and 70 °C and ambient temperatures between -14 °C and 22 °C. The experimental results highlight the importance of installing a variable restrictor on the solution branch to improve performances at partial load, optimizing the generator temperature. The newly designed prototype proved to perform smoothly and to maintain stable operation under the tested steady-state and transient conditions.

© HPC2023.

Selection and/or peer-review under the responsibility of the organizers of the 14th IEA Heat Pump Conference 2023.

Keywords: Absorption Heat Pump; Ammonia; Variable Valves; Gas-fired Generator; Residential Heating

1. Introduction

Absorption heat pumps are a reliable and efficient technology as demonstrated by several applications in the light commercial sector where thousands of gas-driven absorption heat pumps (GHP) are used for many years [1]. This technology is also interesting for the residential market to replace condensing boilers in not or poorly insulated buildings, with high temperature emission systems as radiators, a building typology which represents a large share of the existing European residential buildings [2]. In fact, absorption heat pumps achieve high supply water temperatures with limited performance degradation. For this type of buildings, it has been calculated that absorption heat pumps can provide also higher performances than electric vapor compression heat pumps [2], especially in cold and very cold climates where the COP is reduced by the low outdoor air temperature [3]. Furthermore, the possibility to run absorption heat pumps with green hydrogen or a mix of natural gas and hydrogen, can support the decarbonization of the heating sector, handling the peaks of demand without impacting on the electric grid [1], [4]. Experimental tests confirmed that absorption heat pumps provide higher performances than conventional space heating and water heaters appliances. In [5] two prototypes with a nominal capacity of 23.5 kW have been tested and a Seasonal gas utilization efficiency of 1.36 (based on gross calorific value) has been achieved, considering the climate region IV of the American and Canadian Standard [6]. The seasonal gas utilization efficiency (SGUE) is calculated as the ratio between the useful heat provided by the heat pump during the heating season and the natural gas input. For domestic hot water production (DHW), a 9-month field test has been performed in [7] achieving interesting energy savings, compared to traditional gas tank water heaters. Then, an 18-kW absorption heat pump has been also

* Corresponding author. E-mail address: lorenzo.pistocchini@polimi.it

tested obtaining a Season Gas Utilization Efficiencies of 1.43, 1.38, and 1.24 (all based on gross calorific value) for the warm, average, and cold climates respectively [8], as defined by the European Standard [9] test conditions.

Even if gas-driven absorption heat pumps are a viable alternative to condensing boilers, especially for single or two-family houses with space availability for an outdoor installation, the limited number of manufacturers and the relatively high purchase costs of commercially available heat pumps limit a wide diffusion of this technology [3]. Many different absorption cycles are available, the most suitable ones for the residential sector are the single effect cycle (SE) and Generator Absorber eXchanger cycle (GAX) [10]. The GAX is considered one of the most suitable cycles for residential application because it achieves high performances providing the possibility to heat up the rich solution by recovering part of the heat released in the absorber [11]. To perform this heat recovery, an additional component is needed compared to the single effect cycle. However, the GAX effect is affected by high thermal lift and partial load operation, condition often found in residential applications [5]. Moreover, small-capacity heat pumps in real applications experience frequent load variation and different operating conditions, such as changes in inlet/outlet temperatures, mass flow rates, external temperatures etc. [12]. To improve the performances at partial loads, an optimization of the temperature of the generator is essential. This task can be achieved controlling the weak solution mass flow rate with a variable restrictor in the solution branch [13].

In this project, a compact and cost-effective air-source gas-driven ammonia-water absorption heat pump based on the single effect cycle has been developed and tested. The heat pump is the second-generation prototype of a previous concept, where several innovations have been introduced in the generator (under patent pending), optimized plate heat exchangers have been selected and the variable restrictors for both solution and refrigerant branches have been used. The solution pump is an oil driven diaphragm pump specifically designed for this application. After a description of the prototype, in this work the achieved energy performances are presented and analyzed. Seasonal gas utilization efficiency and other relevant working conditions are shown, highlighting the impact of the use of a variable restrictor to assure efficient operation, and giving evidence of the smooth and stable operation of the heat pump under both steady-state and transient conditions.

2. Prototyping and thermodynamic cycle

In this section the thermodynamic cycle and the peculiarities of the prototype are described.

2.1. Thermodynamic cycle

The small-capacity gas driven absorption heat pump analyzed in this study has been designed for residential and small commercial applications. The single effect cycle shown in Figure 1 has been selected to meet the requirements of this application, strongly driven by space-saving, by the purchase cost for what concerns the economic aspects, and by a wide range of operating conditions for what concerns the technical considerations.

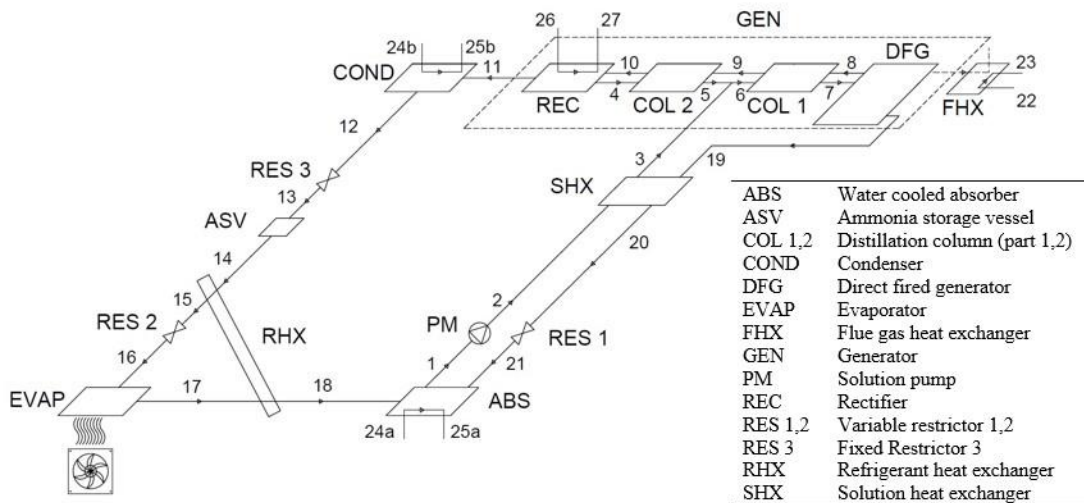


Figure 1: Single effect thermodynamic cycle

The Single effect cycle is composed by the refrigerant and the solution branches. The refrigerant branch is the left side of the cycle in Figure 1 and it is composed by the condenser (COND), the restrictors (RES 2 and RES 3), the refrigerant heat exchanger (RHX), the Ammonia Storage Vessel (ASV) and the evaporator (EVAP). On the other side, the solution branch is composed by the water-cooled absorber (ABS), the solution pump (PM), the restrictor (RES 1), the solution heat exchanger (SHX) and the generator (GEN) that can be divided in the direct fired generator (DFG) directly connected to the distillation column (COL1+COL2) and the water-cooled rectifier (REC). The combustion of natural gas heats up the ammonia-water pool boiling solution in the direct fired generator creating vapor (point 8). The ammonia mass fraction of the vapor is increased, while its temperature is decreased in the first section of the distillation column (COL1) where it flows counter-current with the rich solution (point 6) (high ammonia mass fraction), promoting an intense heat and mass exchange. On the contrary, the rich solution reduces its ammonia mass fraction while increasing its temperature. Since a high ammonia mass fraction ($\approx 99\%$) of the outlet vapor from the generator (point 11) is needed, a partial condensation takes place in the water-cooled rectifier (REC). Between REC and COL1 there is the second section of the distillation column (COL 2), where the vapor (point 9) meets the liquid produced by the partial condensation (point 4). The outlet vapor (point 11) flows toward the condenser where it is cooled down, providing part of the useful effect, and it is throttled in RES 2 and RES 3. Between the two restrictors there is the ASV that stores/releases the refrigerant when it is required, as described in [1], and the RHX that provides an internal heat recovery between the outlet liquid refrigerant of the ASV (point 14) and the outlet vapor of the evaporator (point 17). The weak solution (point 19) (low ammonia mass fraction) leaves the generator, it is throttled in RES 1 and flows to the absorber (point 21) where it is mixed with the refrigerant (point 18) providing part of the useful heat thanks to the exothermic absorption process. The rich solution (point 1) is pumped up by the solution pump (point 2) and it is heated up (point 3) by the weak solution (point 20) in the SHX providing a remarkable internal heat recovery. Then, the rich solution flows in the generator. Looking at the water circuit, the useful effect of the heat pump is provided by the flue gas heat exchanger (FHX), the condenser, the absorber, and the water-cooled rectifier. The water is pre-heated by the FHX cooling down the flue gas (point 23) and compensating part of their humidity content, then condenser and absorber are connected in parallel (point 24a and point 24b). To conclude, the whole mass flow rate flows in the REC (point 26) providing the cooling for the rectification process.

2.2. Prototype description

The sealed circuit of the 10-kW air-water gas-driven absorption heat pump under analysis is shown in Figure 2. To achieve high performances reducing the manufacturing costs, the design of this prototype is based on a mix of standard components available on the market and customized components.

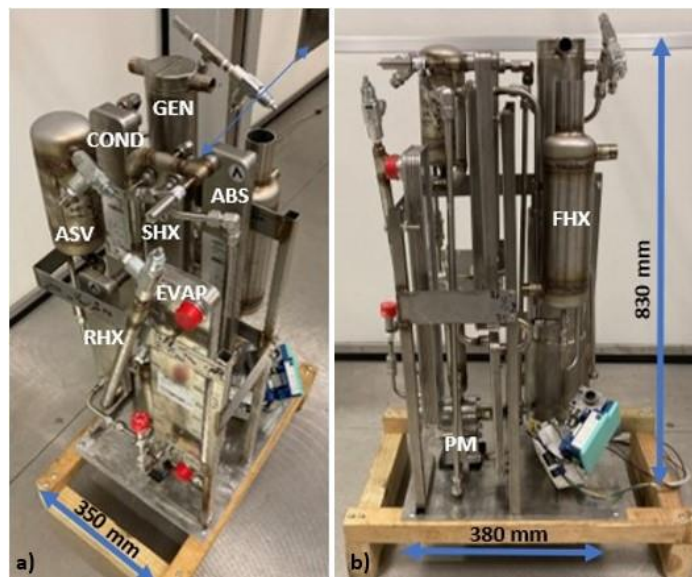


Figure 2: Two side of the GHP sealed circuit, showing its main components and overall dimensions

The customized components are the generator (under patents pending) and the solution pump, i.e. an oil driven diaphragm pump specifically designed for this application, in order to manage the very low flow, the high head pressure, and especially to ensure the complete tightness and maintenance-free reliability in the long term.

The generator has a fire-tube configuration with an innovative geometry that promotes an intense heat exchange between the flue gas and the ammonia water solution maintaining a compact size and reducing the risk of hot spots and local corrosion.

For what concerns the design of the heat exchangers delivering the useful effect of the heat pump, the high difference between the ammonia-water solution mass flow rate and the water mass flow rate represents the most critical issue [1]. In this prototype, standard and custom plate heat exchangers (PHE) developed by Swep have been used. Where possible, an All-Stainless Steel product has been selected, as for the evaporator. When the required All-Stainless Steel PHE is not available, the nickel brazed stainless steel plate PHE has been selected, considering that the corresponding All-Stainless Steel version can be later implemented and produced at a lower cost once you get from GHP prototype to a commercial product.

The solution heat exchanger (SHX) is characterized by a very long thermal length, in order to transfer most of the heat from the weak solution leaving the generator to the rich solution entering the generator. To achieve such a result a multi-pass PHE with a custom configuration has been selected.

The absorber (ABS) consists of two PHE in series, to achieve the required thermal length and manage the different volumetric flow in the refrigerant side, which is mainly a vapor stream at the inlet and a liquid flow at the outlet.

In the evaporator (EVAP) a brine loop (actually filled by a water-glycol mixture) transfers the heat from the outdoor air to the evaporator. This layout may cause a slightly reduction of the performances of the heat pump due to the additional temperature difference caused by use of the intermediate brine loop, however, it offers higher flexibility in installing the sealed circuit indoor and the air heat exchanger outdoor. Furthermore, this option reduces the heat losses towards the environment, partially compensating the performance reduction. Moreover, the use of a brine-water plate heat exchanger as evaporator reduces the internal volume of the sealed circuit, leading to an ammonia content lower than 2 kg, and the risk of refrigerant store-out from the generator into a fin type air-solution heat exchanger, as in case of direct expansion heat pump, during switching on and transients. In addition, thanks to this layout, different defrosting strategies can be implemented. The combination of a compact generator with the use of plate heat exchangers allows for a design of the heat pump able to keep the weight at about 70 kg and to maintain the dimensions close to the ones of a condensing boiler, i.e. 380 x 350 x 830 mm (excluding the outdoor air-brine heat exchanger), as shown in Figure 2. Small capacity heat pumps installed in residential sector works in a wide operating range and under frequent load transient and variable conditions, thus a flexible design under the operating conditions point of view is essential. To achieve this goal, variable restrictors are installed in the solution branch (RES 1) and in the refrigerant branch (RES 2). In contrast, RES 3 is a fixed restrictor that improves the stability of the thermodynamic cycle by introducing a small pressure drop and an intermediate pressure for the ASV and the liquid side of the RHX. The solution branch variable restrictor provides the possibility to optimize the temperature at the base of the generator controlling the flowrate in the solution branch, while RES 2 controls the evaporation temperature to avoid the flooding of the evaporator. The ASV is installed between RES 3 and the RHX to optimize the operation of the RHX [1].

3. Test methodology

The gas-driven absorption heat pump prototype has been tested in an accredited laboratory in the brine-to-water configuration. Temperature measurement is made by high accuracy RTD Pt100 Temperature Sensors (4 wire 1/10 DIN), which coupled to a high precision monitoring system and periodically calibrated allow us to reach an accuracy of ± 0.02 K in the whole operating range.

Flow measurement in the water and brine lines is made by electromagnetic flowmeters, which are periodically calibrated and guarantee 0.1 % of reading accuracy.

Even the particular oil filled volumetric gas flowmeter is periodically calibrated and guarantee 0.5 % of reading accuracy in a wide range of flow rates.

To simulate the impact of the brine loop that transfers heat from the outdoor air to the evaporator, the inlet temperature of the brine is considered 2 K lower than the temperature of the air, with a temperature variation in the evaporator of about 3 K. Consequently, once the ΔT required for the heat transfer between brine and refrigerant is taken into account, the evaporation temperature is about 8-9 K lower than the air temperature, a reasonable value which can be matched when an actual well-designed air-to-brine heat exchanger is used. The

energy performance of a gas-driven heat pump is measured as the ratio between the useful heat provided by the heat pump and the natural gas heat input (\dot{Q}_{gas}), which is the measured volumetric flow of methane, corrected on the basis of actual temperature and pressure, times the net calorific value (LHV [MJ/Nm³]). This ratio is the Gas Utilization Efficiency (GUE) and considers as useful effect the heat provided by the condenser (\dot{Q}_{cond}), the absorber (\dot{Q}_{abs}), the rectifier (\dot{Q}_{rec}) and the flue gas heat exchanger (\dot{Q}_{fhx}) as shown in Equation 1. The Seasonal Gas Utilization Efficiency (SGUE) gives an indication about the performance of the heat pump over an entire heating season and it is calculated as suggested by the European Standard EN 12309 [9]. Both GUE and SGUE can be calculated also on the basis of the gross calorific value (HHV [MJ/Nm³]) simply by substituting LHV with HHV in \dot{Q}_{gas} calculation. The Standard gives the possibility to calculate the SGUE for three different outdoor design temperatures (T_{design}), 2 °C, -10 °C, and -22 °C, that correspond to the three reference climates for Europe, i.e. warm, average, and cold respectively. For each climate, four different climatic curves are available related to low temperature, medium temperature, high temperature and very high temperature applications, to consider different emission systems, i.e., underfloor system, fan coil system, radiators, and high temperature radiators. To define the inlet water temperature, a maximum temperature difference between inlet and outlet temperatures (ΔT_{max}) is calculated by Equation 2 as function of the outlet water temperature (T_{w-out}) [9]. The Standard proposes a calculation method for the SGUE based on the bin method, as for Equation 3, considering the GUE at different load ratios. The partial load ratio (PLR) is calculated as function of the design temperature and the water outlet temperature (T_j) (see Equation 4) assuming that the heating demand of a building decreases linearly with the outdoor air temperature and it is zero when the outdoor air temperature is 16 °C. In this paper, the average climate ($T_{design} = -10$ °C) and the high temperature climatic curve, with 55 °C as supply water temperature at design condition (for radiators), have been selected to optimize the initial charge of ammonia and water. For the average climate, the Standard prescribes to measure the GUE under the working conditions in Table 1 for the high temperature climatic curve. Moreover, the seasonal efficiency of the heat pump to deal with the very high temperature application (see Table 2) has also been tested.

$$GUE = \frac{\dot{Q}_{cond} + \dot{Q}_{abs} + \dot{Q}_{rec} + \dot{Q}_{fhx}}{\dot{Q}_{gas}} \quad (1)$$

$$\Delta T_{max} = 7 + \frac{T_{w-out} - 35}{30} * 10 \quad (2)$$

$$SGUE = \frac{\sum_{j=1}^N h_j * \dot{Q}_h(T_j)}{\sum_{j=1}^N h_j * \frac{\dot{Q}_h(T_j)}{GUE(T_j)}} \quad (3)$$

$$PRL(\%) = \frac{T_j - 16}{T_{design} - 16} * 100 \quad (4)$$

Table 1: Working conditions for the high temperature climatic curve and average climate

	Partial Load Ratio	Reference air temperature	Inlet temperature of brine	Inlet temperature of water	Outlet temperature of water
Conditions	PLR	T_{air}	T_{brine_in}	T_{w_in}	T_{w_out}
-	%	°C	°C	°C	°C
1	100	-10	-12	41.3	55
2	88	-7	-9	39.3	52
3	54	2	0	32.7	42
4	35	7	5	28.7	36
5	15	12	10	24.7	30

Table 2: Working conditions for the very high temperature climatic curve and average climate

Conditions	Partial Load Ratio PLR %	Reference air temperature T_{air} °C	Inlet temperature of brine $T_{brine,in}$ °C	Inlet temperature of water $T_{w,in}$ °C	Outlet temperature of water $T_{w,out}$ °C
1	100	-10	-12	48.0	65
2	88	-7	-9	45.3	61
3	54	2	0	37.3	49
4	35	7	5	32.0	41
5	15	12	10	26.0	32

4. Results

In this section, the experimental results at different working conditions are introduced. Moreover, the additional flexibility provided by variable restrictors is shown.

4.1. Use of valves to control the cycle

The gas-driven absorption heat pump prototype under analysis has variable restrictors for both the solution (RES 1) and the refrigerant (RES 2) branches (see Figure 1). The variable restrictor RES 2 provides the possibility to optimize the evaporation temperature defined as the inlet temperature at the evaporator (point 16), while RES 1 provides the possibility to optimize the temperature at the bottom of the generator.

Figure 3 shows the evaporation temperature variation due to actions on the RES 2 valve. Increasing the aperture of the valve, the evaporator pressure and temperature increase (from point A to point D). This is achieved thanks to an increase of the refrigerant mass flow rate, which reduces the amount of liquid ammonia stored in the receiver and make it available to the thermodynamic cycle. This is normally associated to a lower thermal lift and higher concentration of the rich solution, both beneficial for the efficiency. The higher efficiency is visible from the increase of the difference between inlet and outlet temperatures of the brine circuit. However, when the aperture of RES 2 exceeds its optimal point, the difference between the evaporator temperature and the brine temperature decreases, causing a partial evaporation, which results in the flooding of the evaporator (point E). This phenomenon reduces the heat exchange with the low temperature source and the outlet evaporator temperature decreases. For the selected cycle layout, with the ASV between the condenser and the RHX, a flooded evaporator increases the heat transfer process in the RHX, leading to a higher degree of subcooling in the refrigerant entering the expansion valve. This further increase the flow rate, leading to a deterioration of the performances at the beginning and an interruption of the thermodynamic cycle if this condition persists. To restore a complete evaporation, RES 2 is closed (point F) reducing the refrigerant mass flow rate. As the refrigerant is stored in the ASV and the evaporator temperature decreases, leading to a complete evaporation of the liquid in the evaporator. Thus, the installation of the ASV before the evaporator on the one hand assures the possibility to control the evaporation pressure to optimize the performances, on the other it is required an active control on the restrictor RES 2 to avoid the flooding of the evaporator.

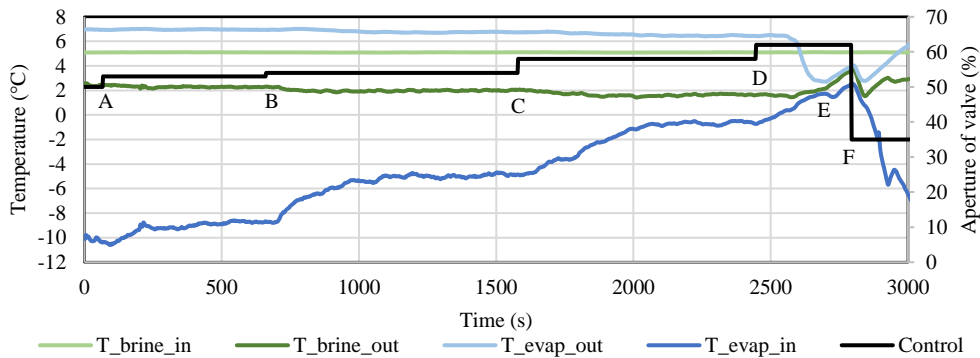


Figure 3: Effect of a variable refrigerant restrictor on the evaporation temperature

Once the control is tuned, the heat pump can operate smoothly and in a stable way under steady-state conditions. This is shown in Figure 4, where inlet and outlet temperatures for both the brine and the refrigerant are reported for a full load (10 kW of heating capacity) condition. The oscillation of all the temperatures is lower than 1 °C with the inlet brine temperature coming from the experimental set-up as the less stable. As for the evaporation temperature, the outlet water temperature variation is lower than 1 °C for the same test (see Figure 5), while the oscillation of the temperature of the weak solution (low ammonia mass fraction) is just slightly higher than 1 °C.

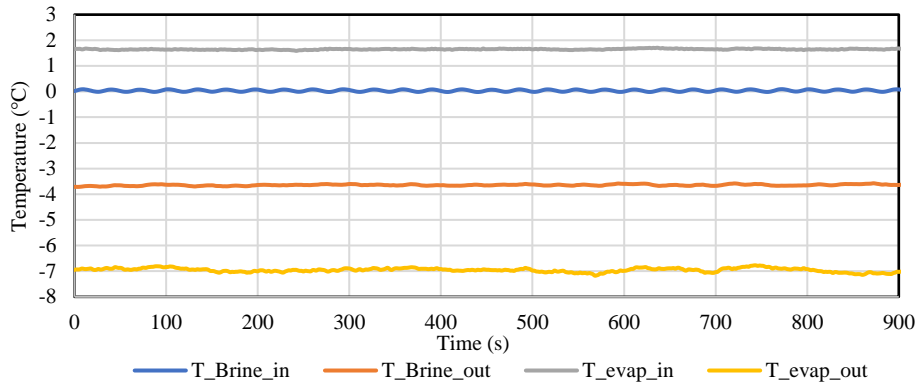


Figure 4: Experimental evaporation and brine temperatures

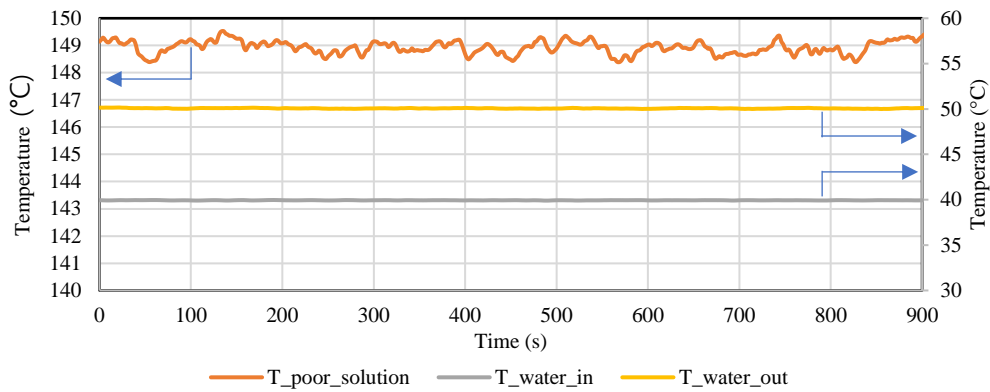


Figure 5: Experimental weak solution and water temperatures

4.2. Seasonal performances

The seasonal performance is calculated in compliance to EN 12309 for the average climate condition, with design temperature of -10 °C, and for the high and very high temperature applications, the former with a nominal supply temperature of 55 °C, the latter with 65 °C, as for the test conditions reported in

Table 1 and Table 2. The actual test conditions for the high temperature application and the measured GUE are reported in Table 3. The resulting Seasonal Gas Utilization Efficiency is 1.58 on a net calorific value basis or 1.42 on the gross calorific value. Table 4 shows the same information for the very high temperature application. Due to the higher supply temperature, the GUEs are lower than for the high temperature application and so is the SGUE, for which a value of 1.51 based on the net calorific value is achieved.

The climatic room where all the tests have been performed has been kept at 20°C, assuming an indoor installation of the GHP.

It must be mentioned that the amount and the average mass fraction of the water-ammonia solution have been optimized for the high temperature application. One of the constraints that have been applied when designing the heat pump and setting the water-ammonia content and mass fraction is that the maximum temperature at the base of the generator should not exceed 180 °C to avoid corrosion issues and assure reliable and safe operation over the entire lifetime. However, given the water-ammonia solution charge set for the high

temperature application, in Condition #1 of the very high temperature climatic curve, the maximum temperature of the generator is reached in correspondence of a heating capacity of 9 kW. Thus, for this application, with the current settings, the design capacity of the heat pumps is reduced from 10 kW to 9 kW, with the part load conditions recalculated accordingly. However, 10 kW could be reached also for the very high temperature application by properly tuning the solution mass fraction and, if needed, changing the RES 1 to increase the maximum flow rate allowed in the weak solution branch.

Table 3: SGUE calculated for high temperature climatic curve for an average climate (EN 12309)

	Useful heat	Inlet temp. of water	Outlet temp. of water	Reference air temp.	Inlet temp. of brine	Outlet temp. of brine	Gas Utilization efficiency
Condition	Q_h kW	T_{w_in} °C	T_{w_out} °C	T_{air} °C	T_{brine_in} °C	T_{brine_out} °C	GUE
1	10.0	41.6	55.5	-10	-12.7	-15.4	1.36
2	9.0	39.4	52.6	-7	-9.0	-12.2	1.41
3	5.3	32.6	41.8	2	0.0	-2.6	1.60
4	3.5	29.0	36.3	7	5.0	2.3	1.67
5	1.6	25.0	30.8	12	10.0	8.4	1.59
SGUE _{Ncv}	-	-	-	-	-	-	1.58
SGUE _{Gcv}	-	-	-	-	-	-	1.42

Table 4: SGUE calculated for very high temperature climatic curve for an average climate (EN 12309)

	Useful heat	Inlet temp. of water	Outlet temp. of water	Reference air temp.	Inlet temp. of brine	Outlet temp. of brine	Gas Utilization efficiency
Condition	Q_h kW	T_{w_in} °C	T_{w_out} °C	T_{air} °C	T_{brine_in} °C	T_{brine_out} °C	GUE
1	9.0	48.1	65.3	-10.0	-12.0	-14.8	1.25
2	7.9	44.9	60.6	-7.0	-9.0	-12.1	1.34
3	4.9	37.2	49.0	2.0	0.1	-2.6	1.54
4	3.2	31.9	40.5	7.0	5.1	3.4	1.57
5	1.3	28.0	32.0	12.0	10.1	8.9	1.46
SGUE _{Ncv}	-	-	-	-	-	-	1.51
SGUE _{Gcv}	-	-	-	-	-	-	1.35

4.3. Full load conditions and low temperature conditions

The heat pump has been tested in different full load conditions as shown in Table 5. The first experimental test (Test #1) has an inlet water temperature of 30 °C and an outlet temperature of 40 °C. This condition is important to test that the compact generator works properly. In fact, the combination of relatively low supply water temperature, which is translated in a reduced high pressure (P_{high}), and the high natural gas heat input, provides an intense boiling process. It may cause the drag of the liquid ammonia-water solution by the vapor stream from the upper part of the generator to the condenser, reducing the performances. In this case, the described phenomenon is not present and a remarkable performance of 1.541 is achieved, with an inlet brine temperature of 0 °C. Then, additional tests are performed increasing the return water temperature, while maintaining the same temperature difference between inlet and outlet water (10 °C). In Test #2, where both inlet and outlet water temperatures were increased by 10 °C compared to Test #1, a decrease of the GUE is measured. Further temperature increase was performed for Test #3 and Test #4 in Table 5, reaching a supply temperature of 65 °C. As expected, the efficiency of the heat pump decreases as the supply temperature is increases, even if the achieved GUE (1.361 with 60 °C as supply water temperature and 1.323 with 65 °C) underline the capability of the heat pump to operate efficiently also at high lift conditions, e.g. when producing domestic hot water (DHW) or when coupled with heating systems that need supply water temperatures higher than the ones considered by the Standard [9]. As additional condition, similar to the ones for domestic hot water production, a higher supply water temperature of 70 °C was set in Test #5, using 15 °C as temperature

difference between supply and return water. Even in this unfavorable condition for heat pumps, the prototype provides an interesting GUE of 1.295, which is about 30% higher than a condensing boiler operating under the same conditions. Since DHW production is usually needed also during mid-seasons and summer, two tests at higher air temperatures (12 °C and 22 °C respectively) are performed. 40/50 °C and 50/60 °C have been used as return and supply water temperatures, simulating two different phases of the charging of the DHW tank. It can be noticed that at higher air temperatures, the low pressure (P_{low}) is higher (4-7 bar), but the thermodynamic cycle works flawlessly, assuring a gas utilization efficiency between 1.45 and 1.60 as shown by Test #6, #7, #8 and #9 in Table 5.

Table 5: Cycle variables and GUE for different full power tests

	Useful heat	Inlet temp. of water	Outlet temp. of water	Reference air temp.	Inlet temp. of brine	Outlet temp. of brine	Inlet temp. of solution at evap.	Pressure at cond. inlet	Pressure at evap. outlet	Gas Utilization efficiency
Test #	Q_h kW	T_{w_in} °C	T_{w_out} °C	T_{air} °C	T_{brine_in} °C	T_{brine_out} °C	T_{evap} °C	P_{high} bar	P_{low} bar	GUE
1	10.2	30.0	40.2	2.0	-0.1	-3.9	-7.3	13.6	2.9	1.54
2	10.0	39.9	50.0	2.0	0.0	-3.6	-7.0	17.6	3.1	1.48
3	10.1	49.9	60.2	2.0	0.1	-3.2	-7.0	22.2	3.0	1.36
4	10.2	55.1	65.4	2.0	0.1	-3.1	-4.9	24.9	3.2	1.32
5	10.0	55.0	70.1	2.0	0.1	-2.7	-4.9	25.2	3.2	1.30
6	10.0	39.9	50.1	12.0	10.1	5.9	2.9	17.8	4.6	1.57
7	10.2	50.1	60.5	12.0	10.1	5.7	3.2	22.8	4.6	1.47
8	10.0	39.9	50.0	22.0	20.0	15.4	12.1	17.9	6.4	1.60
9	10.0	49.9	60.0	22.0	20.1	15.6	13.9	22.9	6.8	1.49

Moreover, the heat pump has been tested at low air temperature, to verify the operation and the efficiency at cold climatic conditions. Test #10 (see Table 6) shows that the heat pump still achieves a GUE of 1.483 with an inlet brine temperature of -16 °C and a supply water temperature of 35 °C, a condition which corresponds to a system with underfloor heating operating at about -14 °C of outdoor air temperature, usually very severe for most of the heat pumps. The minimum temperature considered by the European Standard for a cold climate is -22 °C [9]. This temperature cannot be reached by the calorimeter where the heat pump has been tested in brine-water configuration, due to freezing protection of the glycol circuit. However, to simulate a possible working condition at -22 °C of air temperature, the evaporation temperature was reduced to -30 °C acting on the variable valve on the refrigerant branch (see Test #12 in Table 6). This process replicates very well the operation of a heat pump at -22 °C, except for the temperature of the refrigerant leaving the evaporator. However, this temperature difference has very limited impact in terms of power due to the shape of the enthalpy-temperature curve of the refrigerant in the last phase of the evaporation process. The achieved GUE of 1.429 is remarkable and indicates that the heat pump can work with high efficiency also in the design conditions of the cold climate. Test#12 is performed at higher water and air temperatures where a GUE of 1.309 is obtained with a supply water temperature of 55 °C and an inlet brine temperature of -16 °C.

Table 6: Cycle variables and GUE for low temperature -20°C air 35W tests

	Useful heat	Inlet temp. of water	Outlet temp. of water	Reference air temp.	Inlet temp. of brine	Outlet temp. of brine	Inlet temp. of solution at evap.	Pressure at cond. inlet	Pressure at evap. outlet	Gas Utilization efficiency
Test #	Q_h kW	T_{w_in} °C	T_{w_out} °C	T_{air} °C	T_{brine_in} °C	T_{brine_out} °C	T_{evap} °C	P_{high} bar	P_{low} bar	GUE
10	9.8	26.1	34.9	-14.0	-15.9	-20.3	-25.3	11.8	1.4	1.48
11	9.9	26.1	34.9	-22.0	-15.9	-19.7	-30.0	11.6	1.1	1.43
12	9.9	41.4	55.1	-14.0	-16.0	-19.2	-22.3	17.8	1.6	1.31

5. Conclusions

This work presented the development of a 10 kW single effect ammonia-water gas driven absorption heat pump and its laboratory performances under various relevant operating conditions. The peculiarities of this prototype are the innovative layout of the generator (under patents pending), the use of variable restrictors for both the solution and refrigerant branches, and the use of commercial plate heat exchangers.

The role of the variable restrictors to optimize the low pressure and the efficiency of the cycle was presented, besides a proof of the stable operation of the heat pump. The efficiency of the heat pump was tested in laboratory conditions on a brine-to-water prototype, taking care of simulating the presence of an outdoor air heat exchanger by means of proper settings of the inlet brine temperatures. A remarkable Seasonal Gas Utilization Efficiency equal to 1.58 was achieved in accordance with the European Standard EN 12309 for the high temperature application, with nominal supply temperature of 55 °C, and the average climate condition. Furthermore, a SGUE of 1.51 was reached for the very high temperature application, with 65 °C of nominal supply temperature. Then, the GHP has been tested also in other relevant conditions which demonstrated its capability to provide hot water up to 70 °C and to operate at an equivalent air temperature of -22 °C.

Compactness, high efficiency in all the operation and the flexibility to operate over the wide range of tested conditions demonstrate that the developed heat pump could represent an interesting and reliable solution for space heating and domestic hot water production in residential application.

References

- [1] L. Pistocchini, A. Storoni, T. Toppi, M. Aprile, and M. Motta, "Development of a compact ammonia-water Gas Absorption Heat Pump," in *Proceedings International Sorption Heat Pump Conference 2021 - Part II Call 2021*, 2021, pp. 187–191. [Online]. Available: https://depositonce.tu-berlin.de/bitstream/11303/13495/3/Meyer_etal_Proceedings_2021.pdf
- [2] R. Scoccia, T. Toppi, M. Aprile, and M. Motta, "Absorption and compression heat pump systems for space heating and DHW in European buildings: Energy, environmental and economic analysis," *Journal of Building Engineering*, vol. 16, pp. 94–105, Mar. 2018, doi: 10.1016/j.jobe.2017.12.006.
- [3] M. Garrabrant, R. Stout, M. Blaylock, and C. Keinath, "Residential and Commercial Capacity Absorption Heat Pumps for Space and Domestic Water Heating Applications," *IEA Heat Pump Conference*, pp. 1–12, 2017, [Online]. Available: <http://hpc2017.org/wp-content/uploads/2017/05/O.4.3.3-Residential-and-Commercial-Capacity-Absorption-Heat-Pumps.pdf>
- [4] G. Villa, R. Scoccia, T. Toppi, and M. Aprile, "Energy, environmental and economic analysis of electric vapour compression and gas driven absorption heat pumps for single-family houses," *E3S Web of Conferences*, vol. 312, p. 06001, 2021, doi: 10.1051/e3sconf/202131206001.
- [5] M. Garrabrant, R. Stout, C. Keinath, and P. Glanville, "Experimental Evaluation of Low-Cost Gas Heat Pump Prototypes for Building Space Heating," in *16th International Refrigeration and Air Conditioning Conference*, Jun. 2016. [Online]. Available: <http://docs.lib.purdue.edu/iracc/1573>
- [6] American National Standard/Canadian Gas Association Standard, "ANSI Z21.40.4-1996 Performance Testing and Rating of Gas-fired Air Conditioning and Heat Pump Appliances." 1996.
- [7] P. Glanville, "Field Evaluation of Pre-Commercial Residential Gas Heat Pump Water Heaters," in *ACEEE Hot Water Forum*, Feb. 2016.
- [8] T. Toppi, M. Aprile, M. Guerra, and M. Motta, "Experimental characterization of a newly developed air-source water- ammonia gas absorption heat pump for residential applications," in *International Sorption Heat Pump Conference*, Mar. 2014, pp. 1–10.
- [9] European standard, "EN12309 Gas-fired sorption appliances for heating and/or cooling with a net heat input not exceeding 70kW," 2014.
- [10] B. Dehghan B., T. Toppi, M. Aprile, and M. Motta, "Seasonal performance assessment of three alternative gas-driven absorption heat pump cycles," *Journal of Building Engineering*, vol. 31, p. 101434, Sep. 2020, doi: 10.1016/j.jobe.2020.101434.
- [11] B. A. Phillips, "Development of a high-efficiency, gas-fired, absorption heat pump for residential and small-commercial applications," United States, 1990. [Online]. Available: <https://www.osti.gov/biblio/6004697>
- [12] A. A. Roeder, A. Goyal, and S. Garimella, "Transient simulation of ammonia–water mixture desorption for absorption heat pumps," *International Journal of Refrigeration*, vol. 100, pp. 354–367, Apr. 2019, doi: 10.1016/j.ijrefrig.2019.01.032.
- [13] G. Villa, T. Toppi, M. Aprile, and M. Motta, "Performance improvement of gas-driven absorption heat pumps by controlling the flow rate in the solution branch," *International Journal of Refrigeration*, Sep. 2022, doi: 10.1016/j.ijrefrig.2022.09.015.